Andrzej ŁEBKOWSKI[1]

LIGHT ELECTRIC VEHICLE POWERTRAIN ANALYSIS

Summary. This paper describes the structure of a light electric vehicle known as the Mia Electric vehicle. The vehicle parameters and exploitation properties are presented, while the advantages and disadvantages of the vehicle's technical solutions are discussed, along with possible ideas for their improvement. Vehicle test results on a roller dyno and under actual driving conditions are presented. The data recorded during tests form the basis of an analysis of the vehicle powertrain, whose findings are described in the summary along with testing conclusions.
Keywords: light electric vehicle, EV, BEV, electric powertrain

1. INTRODUCTION

The properties of electric powertrain systems make them a popular choice among car designers to power their creations. At the same time, the thriving era of the large framed cars of the 1970s and 1980s, together with the widespread use of internal combustion engines, is definitely coming to an end. With the advent of modern electric powertrains, a new chapter has begun for automotive technology. Decreasing the mass of a vehicle reduces the amount of energy required to propel it, as well as allows its body to be smaller and lighter. The general aim is to optimize the car construction, while preserving the greatest level of protection for vehicle occupants and other traffic participants. These efforts are augmented by various systems of machine vision and remote vehicle detection [1-6], or autonomous driving systems using data from precise GPS receivers, LIDAR systems or camera clusters installed in

---
[1] Faculty of Electrical Engineering, Gdynia Maritime University, Morska 83 Street, 81-225 Gdynia, Poland. Email: a.lebkowski@we.am.gdynia.pl.

the vehicle [7-12]. Novel construction materials are being engineered, such as aluminium alloys, carbon fibre-reinforced composites and new plastics. These tendencies are present both in conventional cars and in electric or hybrid cars, which exist not because of some short-lived fashion, but because they stem from the necessity to comply with new and increasingly restrictive legislation on permissible vehicle fuel consumption amounts and emission limits [13].

Recently, various models designed in this manner have appeared on the market. One such design was for a vehicle whose production was stopped after 30 months. It was named the Mia Electric (Fig. 1) and is the topic of this article, along with some discussion on possible modifications to it, which could improve its operational adaptability to the northern regions of Europe.

Fig. 1. Mia Electric vehicle

The Mia Electrical vehicle is an example of a futuristic design and worthy of further inspiration, due to its applied engineering. The vehicle parameters make it agile, very ecological and economic, with a unit that is capable of dynamic negotiating with urban areas. The performed tests on the Mia Electric showed that, while it is not without flaws, these can be rectified using simple means. Depending on the selected option, the car's interior can be upholstered with plastic panels and textile fabric or with leather. The view of an example interior is shown in Figure 2.

Fig. 2. Mia Electric interior view [15, 16]

The vehicle construction represents an example of how to design an urban electric vehicle. According to the automotive experts from Carbase [14], by the end of 2014, the Mia Electric was classified as the third (out of 10) best electric vehicle in the world, after the Tesla Model S and the BMW i3. The Mia Electric was regarded as being better overall than other vehicles, such as the Nissan Leaf, the Renault Twizy and Zoe, the Mercedes B-Class Electric Drive, the Smart Fortwo, the Tesla Model X and the Volkswagen e-Golf.

2. BASIC PARAMETERS

Mia vehicles were built in France from June 2011 to December 2013, as typical small urban electric vehicles. There were three body types produced (Fig. 3): the regular Mia (short wheelbase, passenger type, three seats), the Mia U (cargo type or "fourgon", long wheelbase, one or two seats), the Mia L (passenger type, long wheelbase, 3 or 4 seats), and the luxury Mia Paris [15-17]. A total of about 1,950 vehicles was produced at an average rate of 65 units per month.

The Mia Electric vehicle consists of a rigid, light metal structure onto which ABS panels have been glued, forming sides, fenders, bumpers and a roof. Glass panels forming fixed vehicle windows have also been glued directly onto the metal structure (Fig. 4).

On both sides of the vehicle, there are sliding doors with large cutouts in the roof and floor panels, which allow the driver and occupants to freely board and leave, as well as facilitate unobstructed loading and unloading.
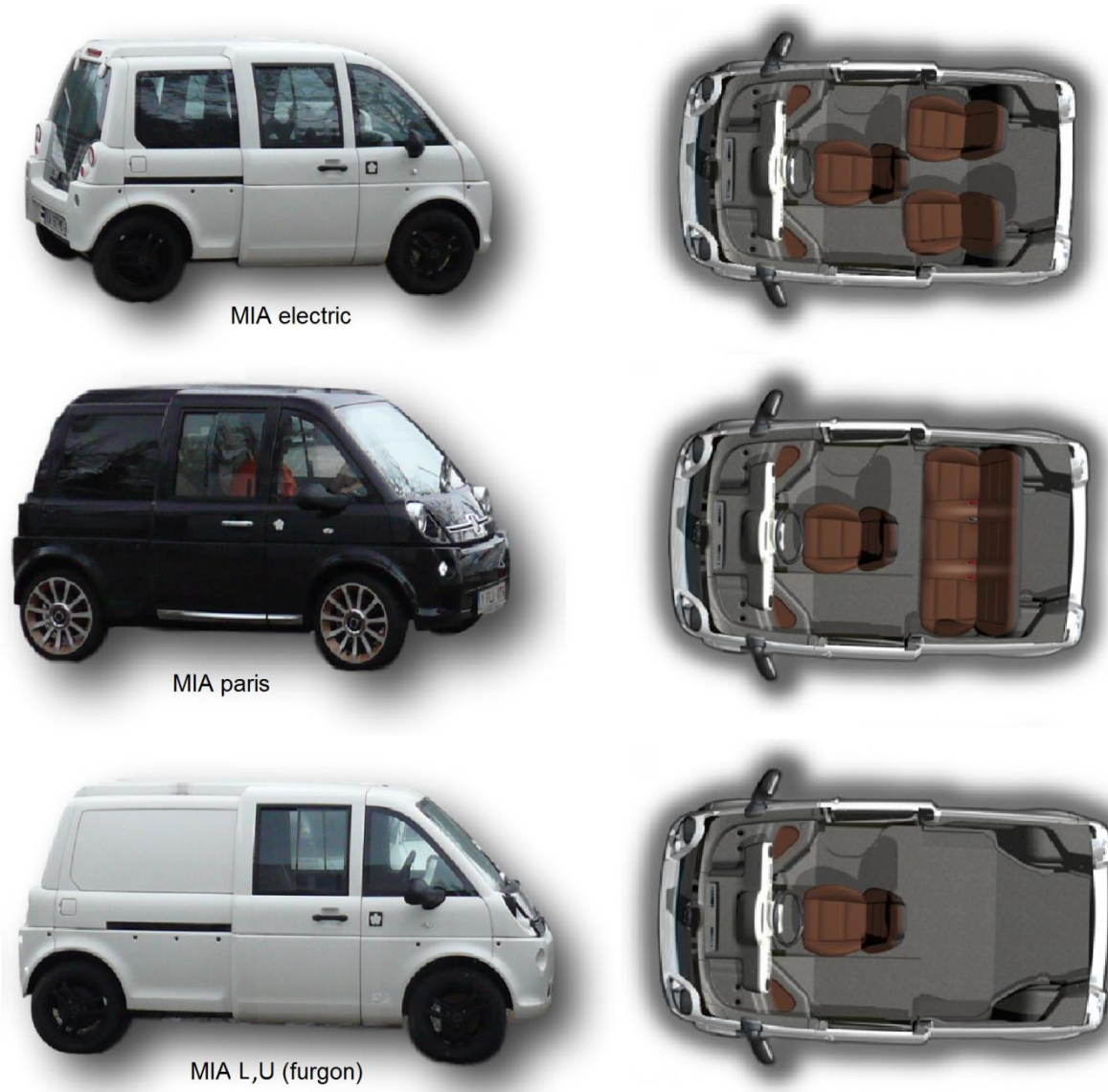
Fig. 3. The tested Mia Electric vehicles

The driver's seat is located centrally on the main axis of the car, which gives the driver a panoramic view of the vehicle's surroundings. Such a layout not only enhances the vehicle's mobility due to an even mass arrangement, but also allows for the use of less precious parking space because, with a centrally placed seat and sliding doors, ingress and egress is possible with minimal spacing in relation to surrounding objects (e.g., parked cars) on the vehicle's sides. The potential for the driver to enter the vehicle from either side also facilitates parking in confined spaces. Behind the driver's seat, depending on the vehicle option, there is cargo space (in the "fourgon" model U), or two single seats (in the Mia, Paris and L models), or one couch with three seats (the L "banquette" model). A particularly ergonomic version of the Mia is one with three seats, i.e., with a central driver's seat and two passenger seats in the rear, where there is generous legroom available to passengers on both sides of driver's seat. The rear of the vehicle contains a tempered glass trunk door, which can be opened by pressing on the key fob or a button on the dashboard.

Fig. 4. The metal structure of the Mia Electric vehicle [17]

The electric powertrain of the vehicle is placed in the rear and consists of an induction motor, powered by a bank of lithium-iron-phosphate (LiFePO4) batteries through an inverter (Fig. 5). The whole powertrain is shielded by an aluminium cowling, shaped in order to direct the airflow around the moving car, which cools the motor and the inverter.
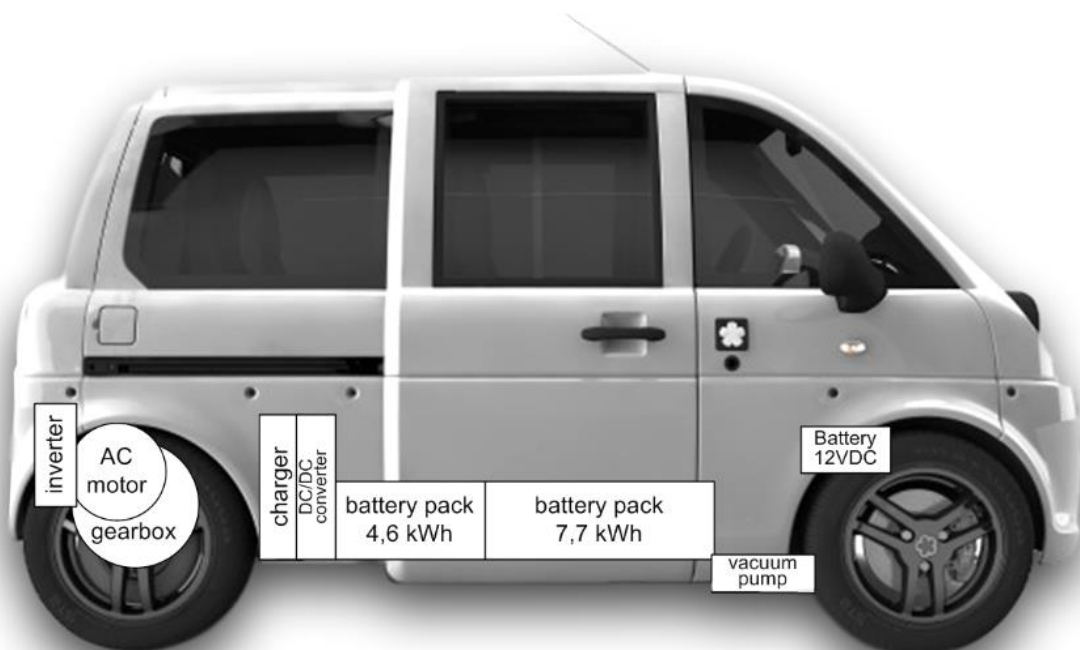

Fig. 5. View of the powertrain from the bottom of the vehicle

On-board auxiliary devices, such as external lights, windscreen wipers, a cabin blower and an electric power braking vacuum pump, are powered from a standard 12 V vehicle supply, which contains a buffer battery with a 17 Ah capacity that is supplied by two parallel DC/DC converters (600 W each) from the high-voltage traction battery. Internal devices communicate with each other using a CAN bus.

The main power source (traction batteries) use LiFePO4 cell chemistry and is divided into two battery packs, located centrally in special compartments at the bottom of the body. Each pack is bolted on top of aluminium panels, which are subsequently bolted to the bottom of the vehicle body. The larger of the battery packs, weighing 92 kg, has a nominal voltage of 48 V, contains 7.7 kWh of power and is installed individually in the front battery compartment located directly under the driver's seat. The smaller battery pack, weighing 55 kg, has a nominal voltage of 28.8 V, contains 4.6 kWh of power and is installed on the aluminium panel, together with two DC/DC converters and the charger, which sits over the converters on a sheet metal riser (Fig. 6). The set consisting of the smaller battery pack, the charger and the DC/DC converters is installed in the rear battery compartment.

Fig. 6. View of the battery packs, the charger and the DC/DC converters

The LiFePO4 battery was built by E4V from 25 cell blocks with a 160 Ah capacity. Each cell block consists of four individual constituent cells, which have a capacity of 40 Ah each. The parameters of each battery block are monitored by a battery management system (BMS) system, also built by E4V. The view of one battery pack with a BMS system is shown in Figure 7.

The BMS system built by E4V belongs to a group of active systems, which use resistor loads to balance the voltage levels on the battery blocks. During charging, when a given block reaches the set voltage, the BMS uses a relay to connect, in parallel, a resistor to that block in order to bypass the majority of charging currents from that block. When all the blocks of a battery reach the set voltage, the BMS sends a command to the charger ordering it to stop charging. Unfortunately, the company that designed the BMS made some design errors, such that, during the life of the vehicle, it is possible that its 12 V auxiliary battery could become completely discharged if the vehicle were to be left unused for a long time. The vehicle designers probably did not foresee the standby charging mode of 12 V from the main traction batteries, when the 12 V battery level becomes low.
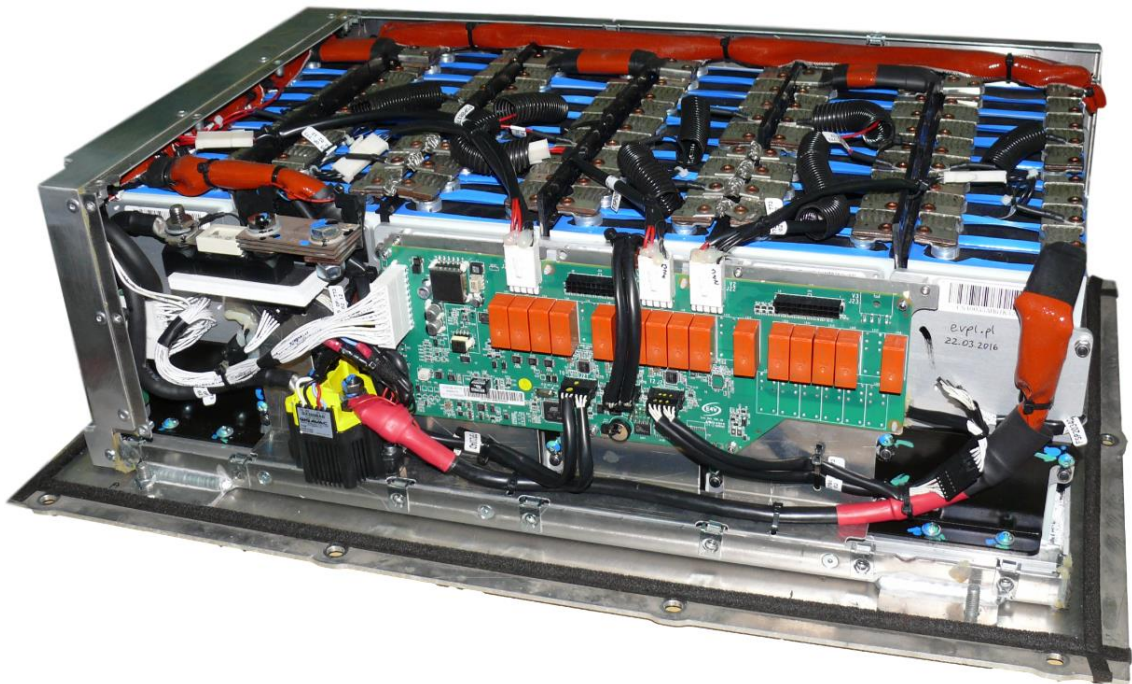
Fig. 7. View of the LiFePO4 battery pack with the BMS board

Furthermore, after a prolonged standstill, the internal BMS components of both battery packs enter a kind of lockdown mode, which puts the vehicle out of commission. Lifting the lockdown is only possible after a costly service. There is, however, an alternative in the form of a firmware modification, performed by direct connection to the CPU of the BMS and by applying the changes to the program memory (Fig. 8).
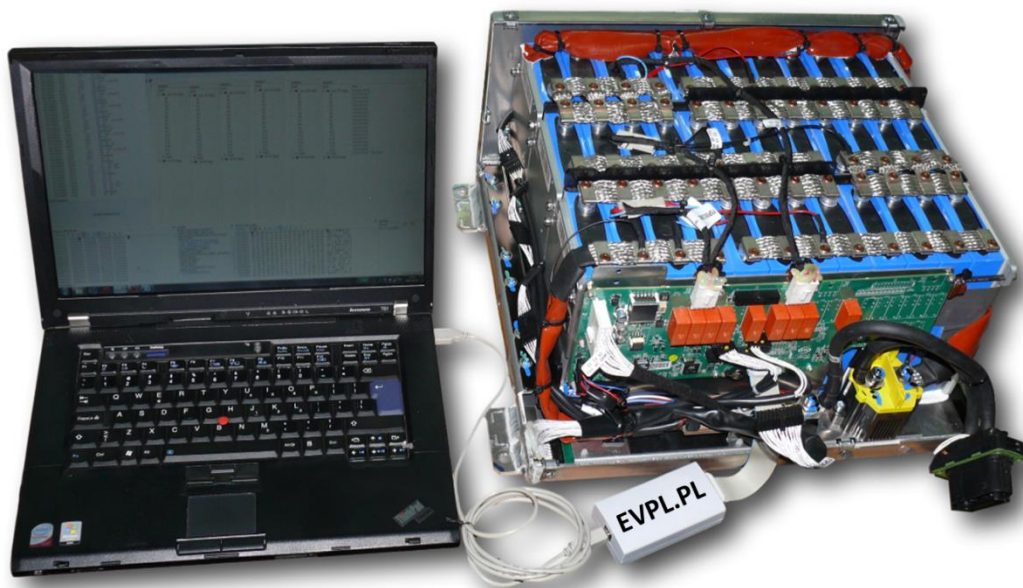

Fig. 8. BMS software modification of a LiFePO4 battery pack

Another obstacle that a user may face during the operation of Mia vehicles is the inability to discharge or charge the batteries when their temperature drops below 0°C. In such a scenario, after turning on the ignition, an indicator lights up on the dashboard informing the driver that the battery system is disabled due to low temperature. The charging is inhibited in the same way: after plugging in the charging cord, the charging will not commence.

The main element of the powertrain is the air-cooled induction motor with a continuous power of 10 kW, weighing 35 kg. It is sourced from Leroy-Somer (a producer of electric motors since 1919 and a supplier of powertrains for Peugeot and Citroën). The motor can be briefly overloaded up to 18 kW, while the maximum motor speed is 9,600 RPM. The IP54 level of protection from water splashes allows for the installation of the motor under the trunk floor, behind the rear fender, as shown in Figure 9.

The torque generated by the motor is transmitted through a single-speed gearbox with a differential to two drive shafts connected to rear wheels [18]. Braking is performed by disc brakes on the front axle and drum brakes in the rear axle, while the braking system is supported by an ABS and an active brake assist (ABA) system. Additionally, the properties of the inverter allow the vehicle to activate regenerative braking at 10% maximum drive torque and a maximum regeneration battery current of 160 A, provided the acceleration pedal is let off, which simulates the response of the conventional drive, but with the advantage of recovering a part of the vehicle's kinetic energy by putting the motor into generator mode and charging the battery as the vehicle brakes. Regenerative braking will not be available when the battery's state of charge exceeds 90% or the battery temperature is close to 0°C.
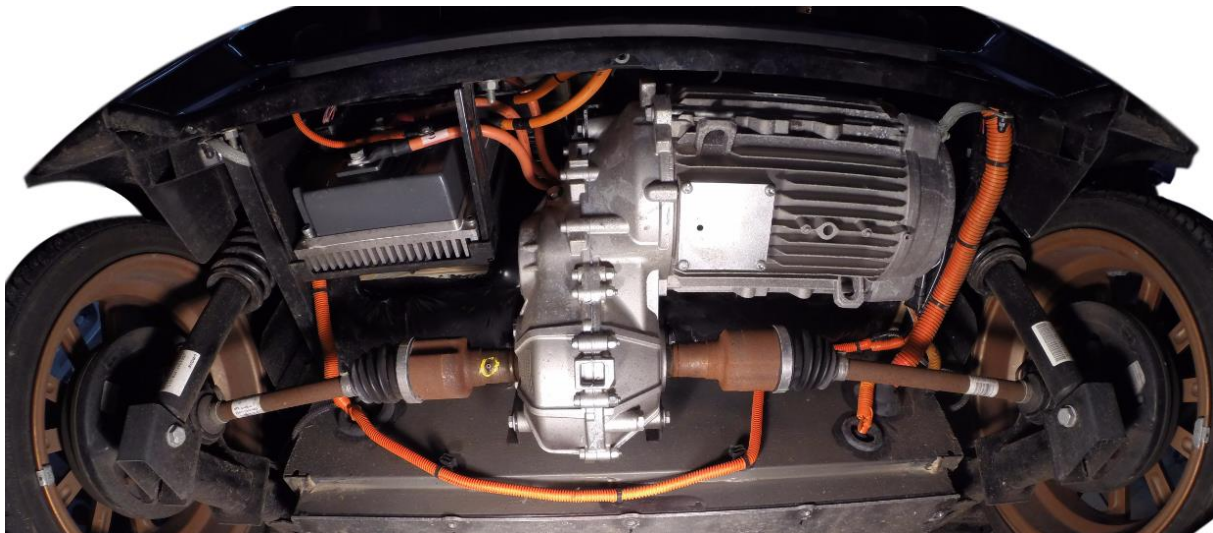

Fig. 9. View of the bottom of the vehicle, with visible powertrain components

The control of the traction motor is performed by the Gen4 Size 4 inverter built by Sevcon. Sevcon inverters are characterized by their compact construction, while retaining the ability to control large powered motors. The Sevcon Gen4 Size 4 inverter, which conforms to the 89/336/EEC Electromagnetic Compatibility Directive, has a mass of 2.7 kg, operating voltage limits from 50.4 to 96 V, a rated continuous RMS current of 140 A and a two-minute rating of 350 A. This means that the inverter is capable of controlling power of about 30 kW. The motor's rotor position is acquired with an incremental encoder with AB output. The inverter uses the field-oriented control algorithm, which allows independent control of motor flux and torque. In order to fully configure the inverter to operate with a given motor, it is required to

set about 280 various parameters, starting with basic motor parameters and finishing with inverter input/output definitions. The inverter allows for configuring selectable drive profiles; the Mia uses two such profiles, namely, regular and ECO. The ECO profile limits the maximum power output, especially during vehicle starting and acceleration.

Table 1. The parameters of the Mia Electric vehicle [15-17]

Index	Name	Data	Unit
1	Dimensions (Mia, Paris)	2,870 x 1,640 x 1,550	(mm)
2	Dimensions (L, U)	3,190 x 1,640 x 1,550	(mm)
3	Wheelbase	1,960	(mm)
4	Turning radius	4.3	(m)
5	Number of seats	1 ÷ 4	(pcs)
6	Battery type	LiFePO4	-
7	Nominal voltage	76.8	(V)
8	Battery energy total	8 or 12.3	(kWh)
9	Battery mass	95 or 145	(kg)
10	Charger type	iSSynergy ELIPS HF65-95V 40A	
11	Approx. battery charging time	3 or 5	(h)
12	On-board charger power	2.4	(kW)
13	DC/DC converter power	2 x 0.6	(kW)
14	Curb weight depending on battery model and capacity	764 ÷ 850	(kg)
15	Gross vehicle weight rating depending on battery model and capacity	1,160 ÷ 1,200	(kg)
16	Motor type	Asynchronous	
17	Motor power	10	(kW)
18	Motor peak power	18	(kW)
19	Motor torque	58 (peak 65)	(Nm)
20	Gearbox	Single speed	
21	Gearbox ratio	8.4 : 1	
22	Inverter	SEVCON Gen4 Size4	
23	Cooling fan (430 m^3/h)	45	(W)
24	Cabin heating power	0.75	(kW)
25	De-icing system power	1.5	(kW)
26	Body structure	Cold-rolled steel closed sections and steel sheet joined by welding	
27	Body skin	ABS	
28	Vehicle range at 15 ÷ 20°C (NEDC)	80 or 125	(km)
29	Top speed	100	(km/h)
30	Specific energy consumption (per km)	96	(Wh/km)
31	Braking system aids	ABS, ABA system	
32	Recycling ratio	95	(%)

An example configuration of motor flux and torque is presented in Figure 10.
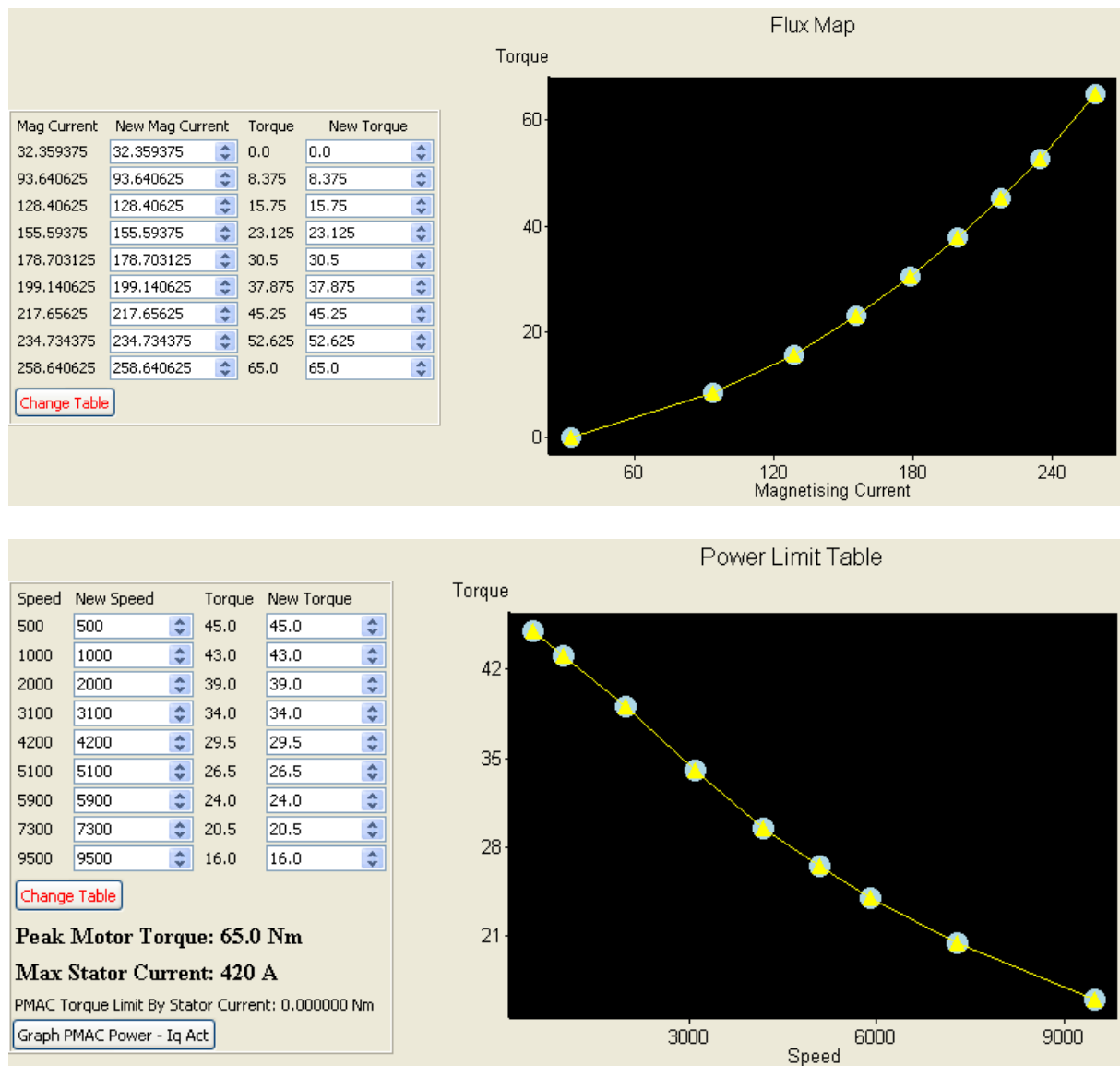

Fig. 10. Inverter configuration of motor flux and torque maps

3. TESTING THE ELECTRIC POWERTRAIN

The electric powertrain tests were conducted under real driving conditions and on a roller dyno. Three Mia vehicles were tested: the regular Mia, the Mia U and the Mia Paris. The test data were recorded with an electric vehicle data recorder [19]. The example data plots recorded during the tests are presented in Figures 11 and 12.
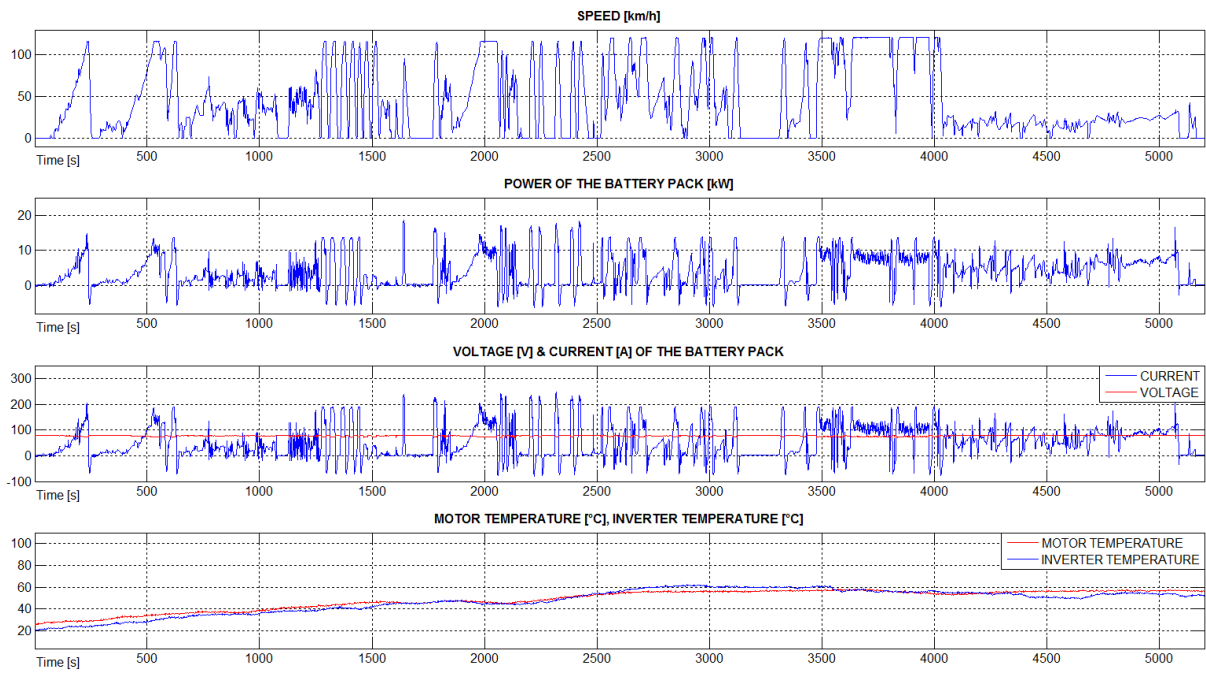
Fig. 11. Plot of example data recorded during the dyno tests of the Mia Electric vehicle
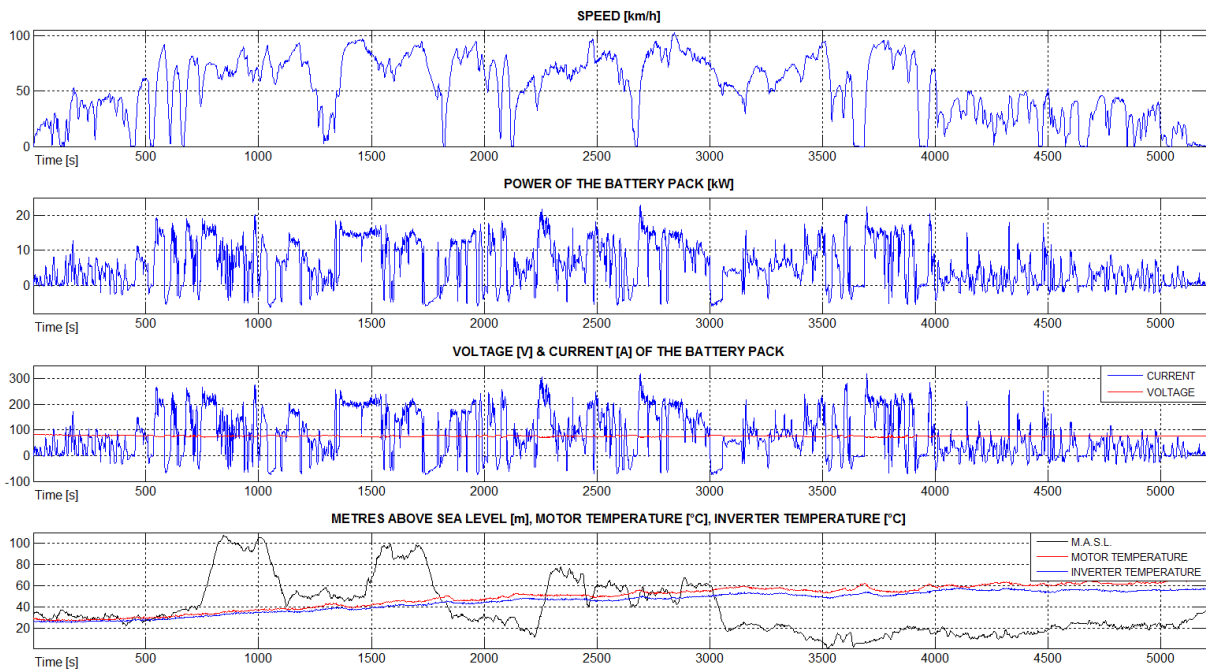

Fig. 12. Plot of example data recorded during the road tests of the Mia Electric vehicle

4. ANALYSIS OF THE RESULTS

During the testing on a roller dyno, the power and torque generated by the powertrain were analysed in relation to the flux map and the power limit table. As aerodynamic drag was not present, the vehicle reached a top speed of 120 km/h, which corresponds to a motor rotation

speed in the order of 9,570 RPM. Exceeding the 9,600 RPM mark would have triggered the overspeed fault and stopped the drive. Changing the settings of power and torque to above 110% of the factory settings value caused excessive temperature rises in both the motor and the inverter.

Testing under road conditions corroborated the very low powertrain energy consumption claims. The measured energy consumption per km in a mixed cycle (urban/extra-urban driving) and at an average ambient temperature of 25°C was 90 Wh/km (compared to the factory claim of 96 Wh/km). Still, the result was achieved in active ECO mode, with an average velocity of 54 km/h at a distance of 120 km (with a maximum top speed of 81 km/h).

Had the ECO mode been inactive, the energy consumption would have been higher because of the faster acceleration of the vehicle. The electric powertrain parameters are sufficient, while the vehicle is not a traffic nuisance; rather, it is quite agile and effortlessly reaches speeds of over 90 km/h, which is the result of a programmed power limit map, where the torque decreases in line with increasing speed.

The top speed achieved during the testing was 102 km/h. The central driver's position in the Mia Electric vehicle is similar to that in a sports car, which can encourage a "sporty" driving style. In this case, the energy consumption can double, increasing even up to 180 Wh/km.

The vehicle operation changes completely during colder seasons. The capacity of the employed LiFePO4 battery is reduced by 8% for each 10°C drop in temperature from the reference value of 20°C [20]. Additionally, the manufacturer did not engineer any thermal conditioning means. In turn, as the battery temperature reaches 0°C, the vehicle battery will neither charge nor discharge rendering the vehicle as useless. During the testing, one of the vehicles was fitted with a custom battery thermal conditioning (heating) system, which eliminated all the problems resulting from a low battery temperature.

The possibility of modifying the unhindered inverter parameters makes the presented energy consumption figures variable, but their values are a direct consequence of driving style (sporty or economic).

The ratio of energy recovered during regenerative braking to energy consumed was about 7.5% (with a setting of 10% braking torque in relation to drive torque). The vehicle is very sensitive to driving style, as well as road conditions (urban or extra-urban).

The test also confirmed the high efficiency of the powertrain, which uses only air cooling. During the tests, temperature rises of no more than 40°C were observed. It is worth noting that the applied motor does not contain any neodymium permanent magnets, which, when subjected to high temperature and high currents, can demagnetize. The maximum power consumption observed during the tests never exceeded 23 kW.

In the tested vehicle, the factory settings of the inverter were correctly chosen, albeit with a slight reserve, which could be utilized with a small change in the settings. The introduced modifications to the BMS firmware, along with installation of a battery thermal conditioning system, have greatly increased the efficacy of the vehicle under low ambient temperature conditions.

5. CONCLUSIONS

Light electric vehicles represent an alternative direction in transport development, especially in larger cities. They use less space, consume a little energy, do not pollute the air and emit almost no noise.

The application of an electric powertrain allows for a reduction in the energy consumption spent on motion to about 100Wh/km in relation to about 350-400Wh/km expended by comparatively sized conventional cars, equating to a consumption of 3-4 l of conventional gasoline or fuel oil.

The decreased energy consumption means decreased costs of operating these electric vehicles, not to mention the lack of regular costs for oil changes or replacing various worn engine components.

With the application of two-way battery chargers, a power flow control and a monitoring system, the presence of a large number of capable electric vehicles should enable the creation of a smart grid with vehicles' batteries acting as a buffer to mitigate the power fluctuations located in the electric grid.

Electric vehicles can substantially reduce the local emission of noxious gasses into the environment, since they emit no exhaust and use no oxygen; their operation is almost neutral to the surrounding environment. In addition, they have a high recycling level (95% in the case of Mia) and emit less noise, especially at velocities of less than 60 km/h, which in turn positively impacts on the general population's health [20-22]. Meanwhile, they generate less vibration than conventional vehicles [23-30].

References

1. Lange Stefan, Ulbrich Fritz, Daniel Goehring. 2016. "Online vehicle detection using deep neural networks and lidar based preselected image patches." *IEEE Intelligent Vehicles Symposium*. DOI: http://doi.org/10.1109/IVS.2016.7535503.
2. Chuanrong Li, Mei Zhou, Liu Menghua, Ma Lian, Wang Jinhu. 2016. "A concealed car extraction method based on full-waveform LiDAR data". *Mobile Information Systems*. DOI: http://doi.org/10.1155/2016/3854217.
3. Yansong Liu, Sildomar T. Monteiro, Eli Saber. 2016. "Vehicle detection from aerial color imagery and airborne LiDAR data." *IEEE International Geoscience and Remote Sensing Symposium (IGARSS)*. DOI: http://doi.org/10.1109/IGARSS.2016.7729354.
4. Michael Kusenbach, Michael Himmelsbach, Hans-Joachim Wuensche. 2016. "A new geometric 3D LiDAR feature for model creation and classification of moving objects." *IEEE Intelligent Vehicles Symposium*. DOI: http://doi.org/10.1109/IVS.2016.7535397.
5. Kenneth Schofield, Mark L. Larson, Keith J. Vadas. 1999. "Display enhancements for vehicle vision system". *US Patent US5949331A*.
6. O'Cualain Diarmad, Martin Glavin, Edward Jones. 2016. "Method for detecting an object in an environmental region of a motor vehicle by means of a camera system of the motor vehicle, camera system and motor vehicle." *US Patent US9340156B2*.
7. Rosolia Ugo, Stijn De Bruyne, Andrew G. Alleyne. 2016. "Autonomous vehicle control: a nonconvex approach for obstacle avoidance." *IEEE Transactions on Control Systems Technology*, Vol. PP, Iss. 99.
8. Boyuan Li, Du Haiping, Li Weihua. 2015. "Trajectory control for autonomous electric vehicles with in-wheel motors based on a dynamics model approach." *IET Intelligent Transport Systems*, Vol. 10, Iss. 5: 318-330. DOI: http://doi.org/10.1049/iet-its.2015.0159.
9. Xiaozhi Chen, Kaustav Kundu, Yukun Zhu, Huimin Ma, Sanja Fidler, Raquel Urtasun. 2016. "3D object proposals using stereo imagery for accurate object class detection." *Computer Vision and Pattern Recognition*. arXiv:1608.07711.

10. Mutz Filipe, Lucas P. Veronese, Thiago Oliveira-Santos, Edilson de Aguiar, Fernando A. Auat Cheein, Alberto Ferreira De Souza. 2016. "Large-scale mapping in complex field scenarios using an autonomous car." *Expert Systems with Applications*, Vol. 46: 439-462.

11. Ingle Shantanu, Madhuri Phute. 2016. "Tesla autopilot: semi autonomous driving, an uptick for future autonomy." *International Research Journal of Engineering and Technology*, Vol. 3, Iss. 9.

12. Le Vinea Scott, Alireza Zolfaghari, John Polak. 2015. "Autonomous cars: the tension between occupant experience and intersection capacity". *Transportation Research Part C: Emerging Technologies*, Vol. 52.

13. "Reduction of pollutant emissions from light vehicles." 2016. Available at: http://eur-lex.europa.eu.

14. "10 of the best electric vehicles". 2016. Available at: http://www.carbase.co.uk.

15. "Mia, the ideal electric car designed for the city." 2016. Available at: mia-automobile-club.com.

16. "Mia electric micro.bus". 2016. Available at: http://www.greencardesign.com.

17. "Mia electric innove pour mieux rebondir". 2016. Available at: http://www.largus.fr.

18. Łebkowski Andrzej. 2017. "Electric vehicle data recorder". *Przegląd Elektrotechniczny*, Vol. 2. ISSN 0033-2097. Doi: http://doi.org/10.15199/48.2017.02.62.

19. Łebkowski Andrzej. 2016. "Temperature, overcharge and short-circuit studies of batteries used in electric vehicles". *Przegląd Elektrotechniczny*. ISSN 0033-2097. (In print).

20. Figlus Tomasz, Jozef Gnap, Tomas Skrucany, Branislav Sarkan, Jozef Stoklosa. 2016. "The Use of Denoising and Analysis of the Acoustic Signal Entropy in Diagnosing Engine Valve Clearance". *Entropy*, Vol. 18, Issue 7: 1-11.
     DOI: http://doi.org/10.3390/e18070253. ISSN: 1099-4300.

21. Kotak B., Y. Kotak. 2016. "Review of European Regulations and Germany's Action to Reduce Automotive Sector Emissions". *European Transport\Trasporti Europei*,
     Issue 61, Paper no 7: 1-19. ISSN: ISSN 1825-3997.

22. Łebkowski Andrzej. 2015. "Emission of noise in electric vehicles". *Economics and Organization of Enterprise*, No.7: 48-62. ISSN 0860-6846.

23. Bensana T., S. Mekhilef. 2016. "Numerical and experimental analysis of vibratory signals for rolling bearing fault diagnosis". *Mechanika*, Vol. 22, No 3: 217-224.
     DOI: http://dx.doi.org/10.5755/j01.mech.22.3.11962. ISSN: 1392-1207.

24. Czech Piotr, Grzegorz Wojnar, Rafał Burdzik, Łukasz Konieczny, Jan Warczek. 2014. "Application of the discrete wavelet transform and probabilistic neural networks in IC engine fault diagnostics". *Journal of Vibroengineering*, Vol. 16, Issue 4: 1619-1639. ISSN 1392-8716.

25. Czech Piotr. 2012. "Identification of leakages in the inlet system of an internal combustion engine with the use of Wigner-Ville transform and RBF neural networks". In Jerzy Mikulski (ed.). 12th International Conference on Transport Systems Telematics. Katowice Ustron, Poland. 10-13 October 2012. Telematics in the Transport Environment. Book Series: *Communications in Computer and Information Science*, Vol. 329: 414-422.

26. Czech Piotr. 2013. "Intelligent approach to valve clearance diagnostic in cars".
    In Bronius Baksys, Algirdas Bargelis, Stasys Bockus, Algimantas Fedaravicius, Vylius
    Leonavicius, Pranas Ziliukas, Romualdas Dundulis, Tilmute Pilkaite (eds.). Proceedings
    of the18th International Conference on Mechanika. Kaunas University of Technology,
    Kaunas, Lithuania. 4-5 April 2013. Kaunas University of Technology. Book Series:
    Mechanika Kaunas University of Technology: 58-61.
27. Louahem M'sabah H., A. Bouzaouit. 2016. "Degradation model of the bearings by
    wiener process". *Mechanika*, Vol. 22, No 3: 225-228.
    DOI: http://dx.doi.org/10.5755/j01.mech.22.3.13000. ISSN: 1392-1207.
28. Madej Henryk, Piotr Czech. 2010. "Discrete wavelet transform and probabilistic neural
    network in IC engine fault diagnosis". *Eksploatacja i Niezawodnosc - Maintenance and
    Reliability*, Vol. 4(48): 47-54. ISSN: 1507-2711.
29. Obuchowski Jakub, Radoslaw Zimroz, Agnieszka Wylomanska. 2016.
    "Blind equalization using combined skewness-kurtosis criterion for gearbox vibration
    enhancement". *Measurement*, Vol. 88: 34-44.
    DOI: http://doi.org/10.1016/j.measurement.2016.03.034. ISSN: 0263-2241.
30. Wodecki Jacek, Pawel Stefaniak, Jakub Obuchowski, Agnieszka Wylomanska,
    Radosław Zimroz. 2016. "Combination of principal component analysis and time-
    frequency representations of multichannel vibration data for gearbox fault detection".
    Journal of Vibroengineering, Vol. 18, Issue 4: 2167-2175.
    DOI: 10.21595/jve.2016.17114. ISSN: 1392-8716.